Powder X-ray Thermodiffraction Study of Mirabilite and Epsomite Dehydration. Effects of Direct IR-Irradiation on Samples

ARTICLE *in* ANALYTICAL CHEMISTRY · JULY 2007

Impact Factor: 5.64 · DOI: 10.1021/ac062412h · Source: PubMed

4 AUTHORS:

Carolina Cardell
University of Granada
42 PUBLICATIONS **481** CITATIONS
SEE PROFILE

A. Sánchez-Navas
University of Granada
36 PUBLICATIONS **406** CITATIONS
SEE PROFILE

F. J. Olmo
University of Granada
166 PUBLICATIONS **2,331** CITATIONS
SEE PROFILE

Daniel Martín-Ramos
University of Granada
40 PUBLICATIONS **453** CITATIONS
SEE PROFILE

Anal. Chem. **2007,** *79,* 4455−4462

Powder X-ray Thermodiffraction Study of Mirabilite and Epsomite Dehydration. Effects of Direct IR-Irradiation on Samples

Carolina Cardell,*,† Antonio Sánchez-Navas,† F. José Olmo-Reyes,‡ and J. Daniel Martín-Ramos†

Department of Mineralogy and Petrology and Department of Applied Physics, Faculty of Science, University of Granada, Avda. Fuentenueva s/n, 18002 Granada, Spain

This paper investigates the thermal and irradiation-dependent dehydration and kinetics occurring in $Na_2SO_4 \cdot 10H_2O$ (mirabilite) and $MgSO_4 \cdot 7H_2O$ (epsomite) at room conditions by using powder X-ray thermodiffraction. An improved version of a first optically stimulated X-ray diffractometer prototype was used. Specific software for the thermodiffraction study was developed (XPowder PLUS) and a filter inserted between the lamp (heating system) and the sample. The results show that these salts are thermal and irradiation sensitive. The temperature and kinetic rates of the salt conversions differed depending on direct exposure to high-intensity radiation (photodehydration) or whether the radiation was blocked by the filter (thermodehydration). In general, radiation-induced dehydration triggers the transformation at lower temperature and accelerates the kinetic reaction more than when the filter is used. Mirabilite dehydration starts with the initial radiation impacts, unlike epsomite. Thermodehydration and photodehydration of mirabilite is a non-isothermal reaction occurring through an amorphous-mediated step. Radiation damage in epsomite leads to isothermal dehydration, whereas non-isothermal dehydration occurs when epsomite is thermally damaged. In both cases, no amorphous material was observed. Because of the weaker bond between cation and oxygen atom in mirabilite, its thermal and radiation stability is lower than in epsomite. These results have important implications for the prevention of salt weathering of porous materials found in the cultural heritage.

Thermodiffraction (XRTD) is a powerful tool used in many research fields of materials science, as well as in the chemical and pharmaceutical industries, metallurgy, geology, archeometry, or planetary science.[1−8] Very different scientific areas such as planetary science, civil engineering, and cultural heritage conservation[9−12] are showing great interest in mineralogical and phase transition of hydrated salts, especially magnesium and sodium sulfates.

Salt crystallization is a ubiquitous phenomenon in nature with significant cultural, social, and economic implications. It is one of the most important causes of deterioration in natural rocks[13−15] and porous materials used in civil buildings and the cultural heritage.[16−19] Alkali sulfates are especially damaging soluble salts found in buildings and decorative materials.[16,19,20] Indeed, sodium and magnesium sulfates are used in accelerated decay tests such as ASTM C88−90 and RILEM PEM/25 to test the durability of building materials.[21,22]

It is recognized that hydrated sulfate salts, and soluble salts in general, are sensitive to temperature (*T*) and relative humidity (RH). Salt weathering in porous materials mainly occurs through repeated crystallization−dissolution or hydration−dehydration that can cause high crystallization pressures in the salt-loaded material leading to its failure.[9] The phase transition reaction can be a highly dynamic process strongly influenced by variation of *T* and RH in

* Corresponding author. E-mail: cardell@ugr.es. Fax: +34 958243368.
† Department of Mineralogy and Petrology.
‡ Department of Applied Physics.

(1) Nordhoff, S.; Ulrich, J. *J. Therm. Anal. Calorim.* **1999**, *57*, 181−192.
(2) García-Guinea, J.; Abella, R.; Sánchez-Moral, S.; Benito, R.; Martín-Ramos, D. *J. Sediment. Res.* **2000**, *70−4*, 964−967.
(3) Bataille, T.; Auffredis, J. P.; Louër, D. *J. Mater. Chem*. **2000**, *10*, 1707−1711.
(4) Correcher, V.; García-Guinea, J.; López-Arce, P.; Gómez-Ros, J. M. *Spectrochim. Acta, A* **2004**, *60*, 1431−1438.
(5) Isnard, O. *J. Optoelectron. Adv. Mater*. **2006**. *8−2*, 411−417.
(6) Vaniman, D. T.; Bish, D. L.; Chipera, S. J.; Fialips, C. I.; Carey, J. W.; Feldman, W. C. *Nature* **2004**, *43*, 663−665.
(7) Linnow, K.; Zeunert, A.; Steiger, M. *Anal. Chem*. **2006**, *78*, 4683−4689.
(8) Wang, A.; Freeman, J. F.; Jolliff, B. L.; Arvidson, R. E. *Lunar Planet. Sci.* **2006**, *XXXVII*, 2168−2169.
(9) Charola, A. E. *J. Am. Inst. Conserv.* **2000**, *39*, 327−343.
(10) Doehne, E. *Geol. Soc. Spec. Publ.* **2002**, *205*, 51−64.
(11) Fortes, A. D. *Axis* **2005**, *1−9*, 1−28.
(12) Martínez-Frias, J.; Amaral, G.; Vázquez, L. *Rev. Environ. Sci. Biotechnol*. **2006**, *5*, 219−231.
(13) Mustoe, G. E. *Geol. Soc. Am. Bull.* **1982**, *93*, 108−115.
(14) Smith, B. J. In *Geomorphology of Desert Environments*; Abrahams, A. D., Parsons, A. J., Eds.; Routledge Chapman & Hall: London, 1994.
(15) McBride, E. F.; Picard, M. D. *Earth Surf. Processes Landforms* **2000**, *25−8*, 869−879.
(16) Schwarz, H. J.; Roesch, H. *Stud. Conserv*. **1993**, *38*, 224−230.
(17) Colston, B. J.; Watt, D. S.; Munro, H. L. *J. Cultural Heritage* **2001**, *4*, 297−307.
(18) Cardell, C.; Delalieux, F.; Roumpopoulos, K.; Moropoulou, A.; Auger, F.; Van Grieken, R. *Constr. Build. Mater*. **2003**, *17*, 165−179.
(19) Thaulow, N.; Sahu, S. *Mater. Charact*. **2004**, *53*, 123−127.
(20) Cardell, C. *Salt crystallization in calcarenites: application to the monastery of Sant Gerome, Granada* (*Spain*); Granada University Press: Granada, 2003 (in Spanish).
(21) ASTM C 88-90, Standard test method for soundness of aggregate by use of sodium sulfate or magnesium sulfate. In *Annual Book of ASTM Standards 4.2*; ASTM International: West Conshohocken, PA, 1997; pp 37−42.
(22) RILEM PEM/25. *Mater. Constr.* **1980**, *17*, 216−220.

10.1021/ac062412h CCC: $37.00
Published on Web 05/15/2007

the surrounding environment.[7,23−26] In fact, many common soluble salts quickly undergo phase transitions in the environmental conditions found in historical buildings.[25,27] Preventive conservation has therefore become a dominant strategy in the management of the cultural heritage in recent years.[28,29] However, the prediction of soluble salt behavior in response to environmental conditions is not straightforward, since not all the factors potentially involved have been considered and studied in depth. Typically, changes in *T* and RH are thought to initiate the deleterious phase transition reaction. This study will show that brief but intense light irradiation also affects the stability of soluble salts. The rate at which phase transitions take place is another crucial parameter determining the magnitude of the damage. In this sense, a salt with a fast response to changes in ambient RH, *T*, or both is considered to be more damaging than a slow one.[26]

Recently, knowledge on hydrated salts has benefited from research in planetary science on these minerals and their phase transition processes, since they are considered targets in the search for life in Mars, and to understand the hydrogeologic history of this planet and chondritic meteorites.[6,8,11,12] The thermal and radiation stabilities of several hydrated salts such as epsomite, mirabilite, natron, and gypsum have been examined for their UV shielding properties with potential to provide a UV screen for life.[12,30]

In the field of cultural heritage, the radiation output of camera flashes in museums and monuments is an issue of major concern and controversy, since they influence the so-called "light life" of an artwork (how much cumulative exposure to light it can withstand before deteriorating). Flash photography is controlled by many museums for reasons of artwork safety. Contradictory opinions are held about the effects of camera flashes on artworks as well as the most appropriate photo lamp to use. It has been suggested that electronic flash (strobe) is the safest lighting for such photography, as tungsten and quartz lamps have very high levels of infrared light causing heat.[31] For many museums, halogen photo lighting is the common method of lighting even when they have a much greater UV and IR output that any electronic flash equipment. For some authors, the short duration of electronic flash, despite its high output of UV and IR radiation, is not excessively injurious for the art work.[31,32] Due to the key role of soluble salts as decaying factors in the cultural heritage, it is crucial to gain knowledge of the complex interactions among salts and the surrounding environment in order to design specific environmental strategies to preserve artworks.

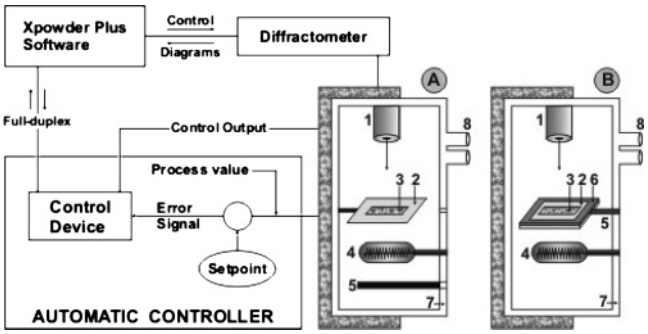

Figure 1. Schematic picture of the modified OSXRD prototype showing the two configurations of elements in the X-ray chamber: (1) X-ray tube, (2) sample holder, (3) sample, (4) lamp, (5) *T* sensor, (6) filter, (7) refrigerated chamber wall, and (8) plugs for cool the refrigeration system.

The dynamics of dehydration is still a poorly understood complex mechanism that this study aims to improve by the following: (i) investigating in situ dehydration of mirabilite and epsomite at room *T* and RH conditions using powder X-ray thermodiffraction to further understand the physicochemical mechanisms involved in the phase transition reactions; (ii) examining the influence and kinetic effects of thermal and radiation stimulation on the dehydration processes; and (iii) explaining the behavior of the crystalline structures of both hydrated salts in thermodehydration and photodehydration experiments.

EXPERIMENTAL SECTION

Powder X-ray Thermodiffraction. Temperature-dependent powder X-ray diffraction was performed by fine-tuning an optically stimulated X-ray diffractometer (OSXRD) prototype described elsewhere.[2] The halogen lamp (heating system; Philips Capsuleline Pro 75 W, 220 V) provides up to 210 °C for the sample. This temperature (*T*) covers the range in which many substances such as hydrated minerals, clays, or organic compounds undergo physicochemical processes such as phase transition, dehydration, crystallinity changes, etc. Thermodiffraction itself starts with several flashes of the light emitted by the lamp, which can be compared to camera flashes. This observation suggested researching the risk of irradiation damaging the studied sulfate salts. Two experiments were carried out based on two configurations of elements in the X-ray chamber (Figure 1). According to the sample−lamp−*T* sensor arrangement (similar distance separates the sample and the *T* sensor from the lamp), the light beam impacts directly on the sample. With the sample−filter/*T* sensor−lamp arrangement, the sample is indirectly lit, receiving less intense light impacts.

A PW1710/00 X-ray diffractometer was used with PW1712 communication card via RS232 serial port, full-duplex controlled

(23) Hamad, S. El D. *Thermochim. Acta* **1975**, *13*, 409−418.
(24) Hamad, S. El D. *Thermochim. Acta* **1976**, *17*, 85−96.
(25) Arnold, A.; Zehnder, K. In *Atti 1° Simposio Intenationale La conservazione dei monumenti nel bacino del Mediterraneo; influenza dell'ambiente costiero e dello spray marino sulla pietra calcarea e sul marmo*; Zezza, F., Ed.; Bari, 1989; pp 31−58.
(26) López-Arce, P.; Doehne, E. In *Proceeding of Heritage, Weathering and Conservation*; Fort, R., Alvarez de Buergo, M., Gómez-Heras, M., Vazquez-Calvo, C. Eds.; Madrid, 2006; pp 285−291.
(27) Siedel, H. In *Proceeding of the 6th International Congress on Applied Mineralogy*; Heimann, R. B.: Göttingen, 2000; Vol. *2*, pp 1035−1038.
(28) Price, C. A.; Brimblecombe, P. In *Preventive Conservation: Practice, Theory and Research*; Roy, A., Smith, P., Eds.; International Institute for Conservation of Historic and Artistic Works: London, 1994
(29) Price, C. A. *An expert chemical model for determining the environmental conditions needed to prevent salt damage in porous materials*. European Commission Research Report 11, Protection and Conservation of European Cultural Heritage: London, 2000.
(30) McCord, T. B.; Orlando, T. M.; Teeter, G.; Hansen, G. B.; Sieger, M. T.; Oetrik, N. G.; Van Keulen, L. *J. Geophys. Res.* **2001**, *106*−*E2*, 3311−3319.
(31) Swann, J. *Guidelines for Costume*; ICOM Costume Committee, 1998; http: dept.kent.edu/museum/link/icom.html.
(32) Brimblecombe, P. In *Cultural Heritage Conservation and Environmental Impact Assesment by non-destructive testing and micro-analysis*; Van Grieken, R., Janssens, K., Eds.; Balkema, A. A. Publishers: Leiden, 2005; pp 11−18.

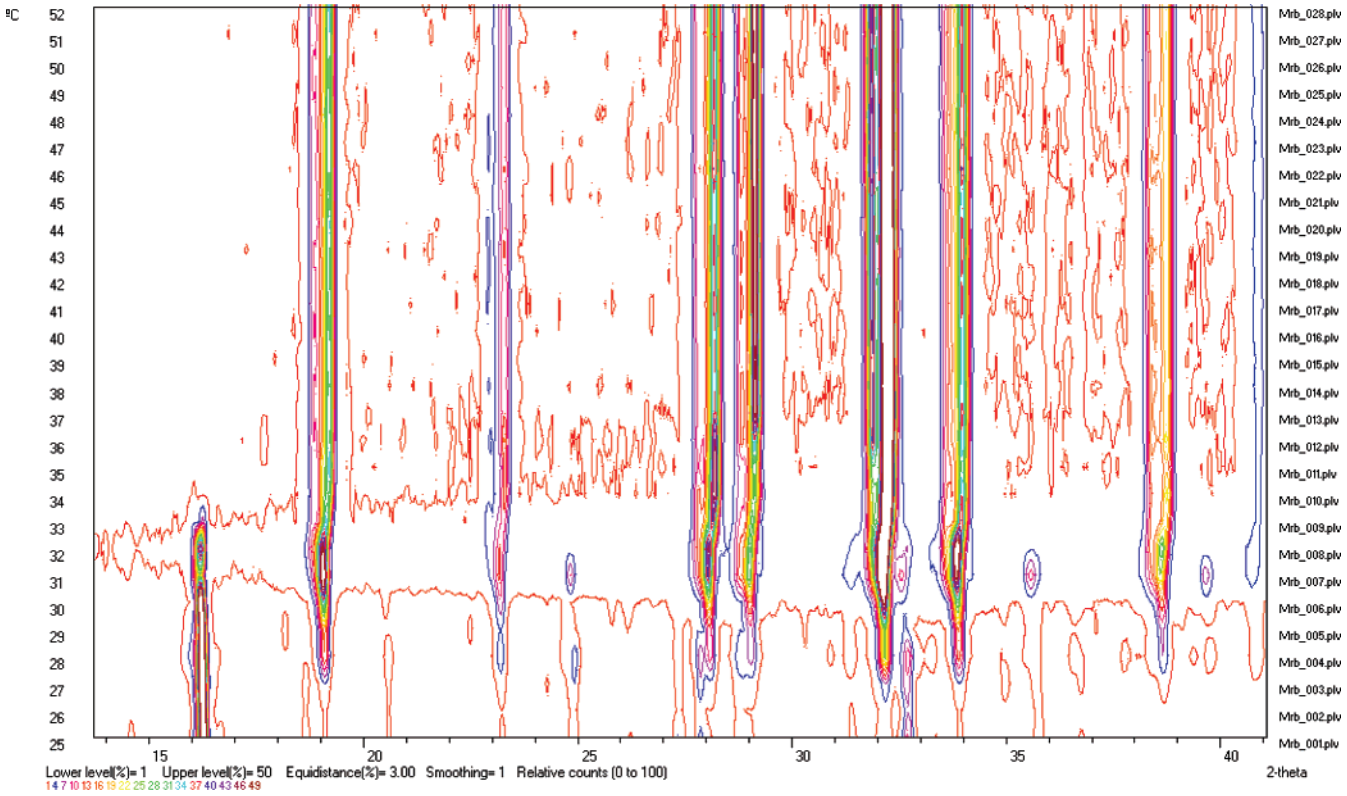

Figure 2. XRTD mapping for mirabilite dehydration obtained with filter. A distinctive XRD line of mirabilite appears at ~16° 2θ, and the strongest diffraction line for thenardite is seen at ~19° 2θ.

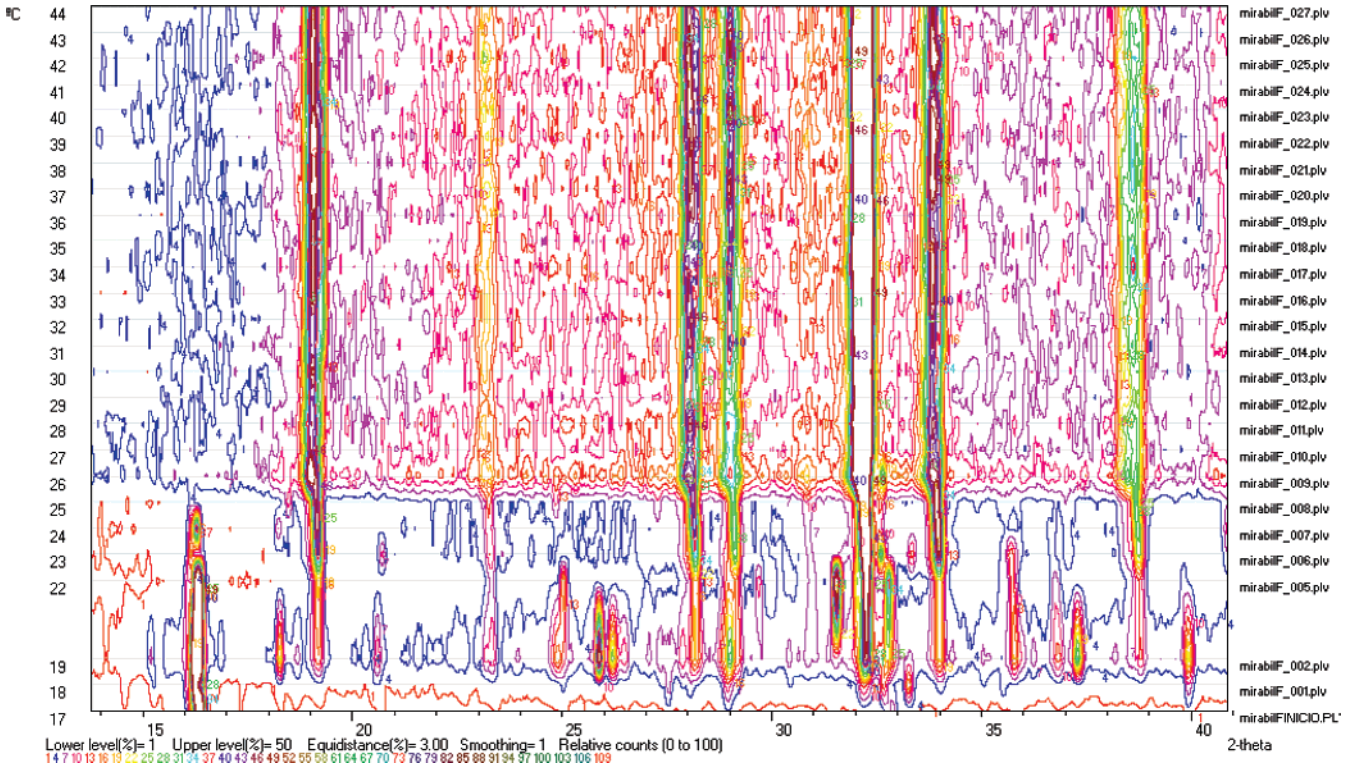

Figure 3. XRTD mapping for mirabilite dehydration obtained using no filter. A distinctive XRD line of mirabilite appears at ~16° 2θ, and the strongest diffraction line for thenardite is seen at ~19° 2θ.

by the XPowder PLUS software particularly developed for this work.[33] The X-ray chamber was cooled by continuous water flow around the chamber walls, the T was monitored (Pt-1000; 0.5 °C precision), and a software-controlled thermostat with digital T selection (control device; Figure 1) precisely regulated lamp heating. Additional innovations were as follows: (1) lamp intensity was not controlled by voltage modulation, but rather according to microshorts (ms in duration) in the otherwise constant 12-V

power; (2) a new door for the X-ray chamber was built with holes to attach the water cooling system, the power wires for the lamp, the T sensor, and the filter especially built for this study (this is a 2 × 2 cm square, 5-mm-thick laminated aluminum plaque with the T sensor inside, as in Figure 1); and (3) to avoid divergent light irradiation on the sample, a new glass sample holder was adapted with a groove of dimensions of 0.5 × 2 × 20 mm to contain the top-loaded sample. The lamp filament was aligned parallel to the sample to minimize T gradients at the sample surface.

Powder XRD data were collected using the Bragg−Brentano focusing geometry with a graphite secondary monochromator, λ-(Cu Kα1) = 1.5406 Å, automatic divergence 1° slit and receiving slit of 1/0.1/1. The XRD patterns were scanned over a $3° < 2\theta < 60°$ range, with 0.1 goniometric rate, 0.4-s integration time, 0.040 step size. Scan mode was continuous. Voltage was 40 kV, and tube current 40 mA. Diffraction patterns were collected in air (~50% relative humidity. RH) from 10-min scans at 1 °C increments between 20 and 60 °C. Temperature in the diffraction chamber was stabilized by a 1-min pause between diffractograms. Isothermal XRD analyses require stable, linear control of T, achieved here by the T control loop system mentioned above. Phase transformations were easily detected by the appearance or disappearance of characteristic peaks in the XRD patterns.

In addition to the 3D images obtained up to now,[2,3,7] the new XPowder PLUS software develops new routines for 2D figures or mapping, which show better the evolution of the physicochemical processes susceptible to monitoring by X-ray diffraction. The only requirement to obtain mappings is that XRD data must be collected with similar λ, $\Delta\theta$, initial 2θ, and final 2θ. Sequential profiles (ASCII file) were obtained (up to 50 diffractograms) and then processed, so that 2D or 3D images were obtained. Automatic acquisition, evaluation, and computation of XRD data were carried out with the XPowder program[33] that also offers tools to automatically measure thermal dilatation coefficients. Linear and volumetric coefficients were calculated from refined lattice parameters at dehydration T and 60 °C.

Spectroradiometer Measurements. The emission spectrum of the halogen lamp at room temperature (±20 °C) was measured using a portable LICOR LI1800 spectroradiometer. This is a single monochromator that can measure the global irradiance in selected spectral bands. We used the measurements taken between 300 and 1100 nm with a full width at half-maximum (fwhm) of ~6 nm and a wavelength step of 1 nm. Absolute accuracy of the irradiance measurements is expected to be better than ±5%. The wavelength accuracy is ±2 nm, and the wavelength repeatability ±0.5 nm.

Materials. Solid crystalline mirabilite and epsomite (Panreac, analytical grade) were used as starting minerals. Powdered samples for analysis were obtained by moderate grinding of the single crystals in an agate mortar. Prior to XRTD analyses, an X-ray diffraction was conducted for both precursors to ensure no phase transition occurred during sample handling, since mirabilite and epsomite dehydrate in dry air.[23,24,26] Precautions were taken to ensure that no transformations occurred. These included the following: (i) the precursors were stored in the refrigerator; (ii) they were lightly ground in the agate mortar (average particle size of ~40−50 μm), since it was observed that intense grinding favored dehydration, as did pressing them in the sample holder. This operation should be done at room T of ~20 °C; (iii) once placed in the glass holder, the samples were stored in the refrigerator and transported to the diffractometer room just before XRTD analysis; (iv) diffractometer room temperature was kept below 20 °C.

(33) Martín-Ramos, J. D. Using XPowder: A software package for Powder X-Ray diffraction analysis. www.xpowder.com D.L.; 2004 (GR 1001/04.ISBN 84-609-1497-6).

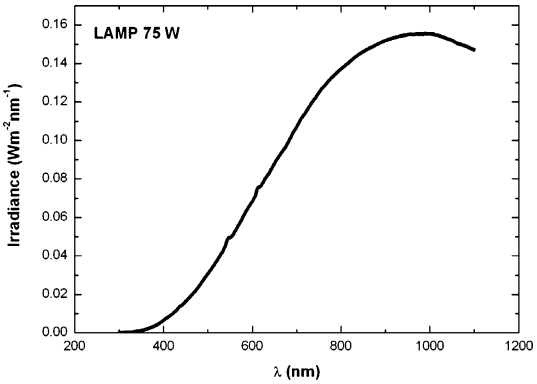

Figure 4. Emission spectrum of the halogen lamp used as heating system in the XRTD.

RESULTS

Mirabilite Dehydration Process. Figures 2 and 3 show the mapping of mirabilite dehydration obtained respectively with and without a filter. Mirabilite was identified using card 75-1077 of the 2003 Powder Diffraction File database and thenardite using card 75-0914. The distinctive diffraction line of mirabilite appears at ~16° 2θ, and the strongest diffraction line for thenardite is seen at ~19° 2θ. Comparison of Figures 2 and 3 shows that in both cases mirabilite dehydration is a non-isothermal reaction. However, the phase transition toward thenardite occurs at different temperatures and rates depending on whether the filter is used or not. The map obtained with the filter (Figure 2) shows that mirabilite dehydration starts at ~27 °C and continues up to ~33 °C. In this range, mirabilite and thenardite coexist, while above 33 °C thenardite is the only mineral present. Figure 2 also shows that during mirabilite−thenardite conversion there is a loss of crystallinity, i.e., presence of amorphous phase, as indicated by the increase in the background shown by the broad horizontal band.

Figure 3 shows that when the filter is not used the dehydration process of mirabilite starts at lower T. Indeed, the results show that the critical T for the onset of dehydration was 18 °C, corresponding to the initial T of the experiment. This important finding indicates that the initial halogen burst (required for the XRTD experiment to start, and prolonged during the 1 min used to stabilize the T chamber) is enough to trigger mirabilite dehydration. To confirm this effect, several XRTD experiments were performed starting between 18 and 21 °C, and in all cases, the transformation began at the initial T of the experiment. To further investigate this radiation-induced dehydration, we measured the emission spectrum of the halogen lamp (Figure 4), which mainly emits in the visible−infrared spectrum, releasing little UV irradiation. The total energy measured was 68.2 W m^{-2}, with a peak at 983 nm, and energy in the UV (300−400 nm) equal to 0.18 W m^{-2}; i.e., less than 1% of lamp emissions are UV. The

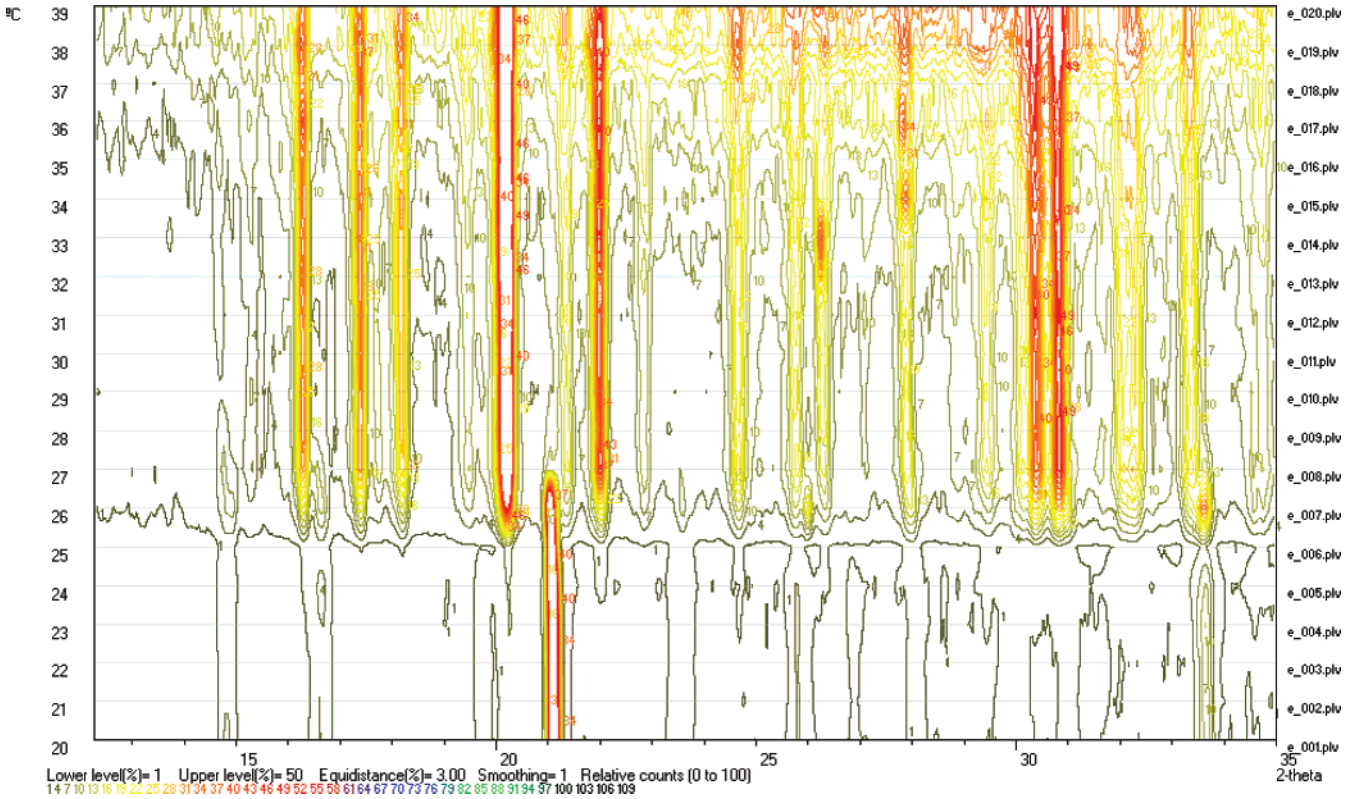

Figure 5. XRTD mapping for epsomite dehydration obtained with filter. The strongest XRD line of epsomite appears at ~21° 2θ; the remaining strong lines above the epsomite line correspond to hexahydrite.

map of Figure 3 shows horizontal bands throughout the mirabilite−thenardite transformation, meaning that amorphous material is also produced in this experiment during phase conversion.

In both XRTD experiments, it was observed that once mirabilite dehydration has concluded, the new anhydrous phase thenardite maintains its crystallinity (i.e., constant mosaic domain) with rising T, as indicated by the constant fwhm of the vertical bands corresponding to successive thenardite peaks (see Figures 2 and 3). However, when the filter is not used, more background is present, as shown by the profuse vertical lines of Figure 3, that must be due to abundant amorphous components.

Epsomite Dehydration. Figures 5 and 6 respectively show the mappings for epsomite obtained with filter and without filter. Epsomite was identified using the 72-1112 card of the 2003 Powder Diffraction File database and hexahydrite with the 72-1068 card. Figure 5 shows that the strongest diffraction line of epsomite appears at ~21° 2θ, while the remaining strong lines above the epsomite line correspond to hexahydrite. Dehydration of epsomite occurs between ~25 and 27 °C, where epsomite and hexahydrite coexist. Thermodehydration of epsomite is therefore a non-isothermal reaction. Above 27 °C, the epsomite transforms completely into the new phase, hexahydrite. During this phase transition, no amorphous material is present as indicated by the absence of background sound (no narrow horizontal band) throughout the transition. The hexahydrite forms and grows rapidly. Nucleation is very fast as suggested by the narrow epsomite and hexahydrite coexistence range of ~2 °C. Figure 5 also shows that above ~37 °C hexahydrite starts to amorphize as indicated by the abundant horizontal bands.

The results of epsomite dehydration without the filter (Figure 6) show that epsomite photodehydration is an isothermal transformation occurring at 28 °C and that during the transformation no loss of crystallinity is found as suggested by the lack of horizontal background sound. Unexpectedly, the T of phase transition was similar with and without use of the filter. However, unlike the anhydrous phase thenardite, the new phase hexahydrite lost crystallinity above ~35 °C, as shown by the absence of constant width vertical bands in Figures 5 and 6. Nonetheless, irradiation without the filter favors abundant production of amorphous components as seen in the more profuse vertical lines in Figure 6.

Volumetric dilatation coefficients have been calculated for thermal expansion of thenardite and hexahydrite as $0.076\,62 \times 10^{-3}$ and $0.147\,38 \times 10^{-3}$ K^{-1}, respectively. Anisotropy was observed in expansion of both minerals, with dilatation coefficients $\alpha_a = 0.039\,13 \times 10^{-3}$ and $\alpha_b = 0.022\,44 \times 10^{-3}$ K^{-1} greater than that along the c-axis ($\alpha_c = 0.014\,88 \times 10^{-3}$ K^{-1}) for thenardite, and $\alpha_a = 0.186\,59 \times 10^{-3}$ K^{-1}, $\alpha_b = 0.113\,26 \times 10^{-3}$ K^{-1}, and c-axis ($\alpha_c = -0.15247 \times 10^{-3}$ K^{-1}) in hexahydrite.

DISCUSSION

Thermodehydration and Photodehydration of Mirabilite and Epsomite. Na_2SO_4 is reported to have five polymorphs, namely, phases I, II, III, IV, and V. Between 20 and 180 °C, phase V is the stable phase.[35,36] Different transition temperatures for mirabilite dehydration are reported, depending on the environmental conditions of the thermal experiments. The mirabilite−

(34) Winkler, E. M. *Stone: Properties, durability in man's environment,* 3rd ed.; Springer-Verlag: Berlin, 1997.
(35) Naruse, H.; Tanak, K.; Morikawa, H.; Marumo, F. *Acta Crystallogr., B* **1987**, *43*, 143−146.
(36) Rasmussen, S. E.; Jørgense, J. E.; Lundtoft, B. *J. Appl. Cryst.* **1996**, *29*, 42−47.

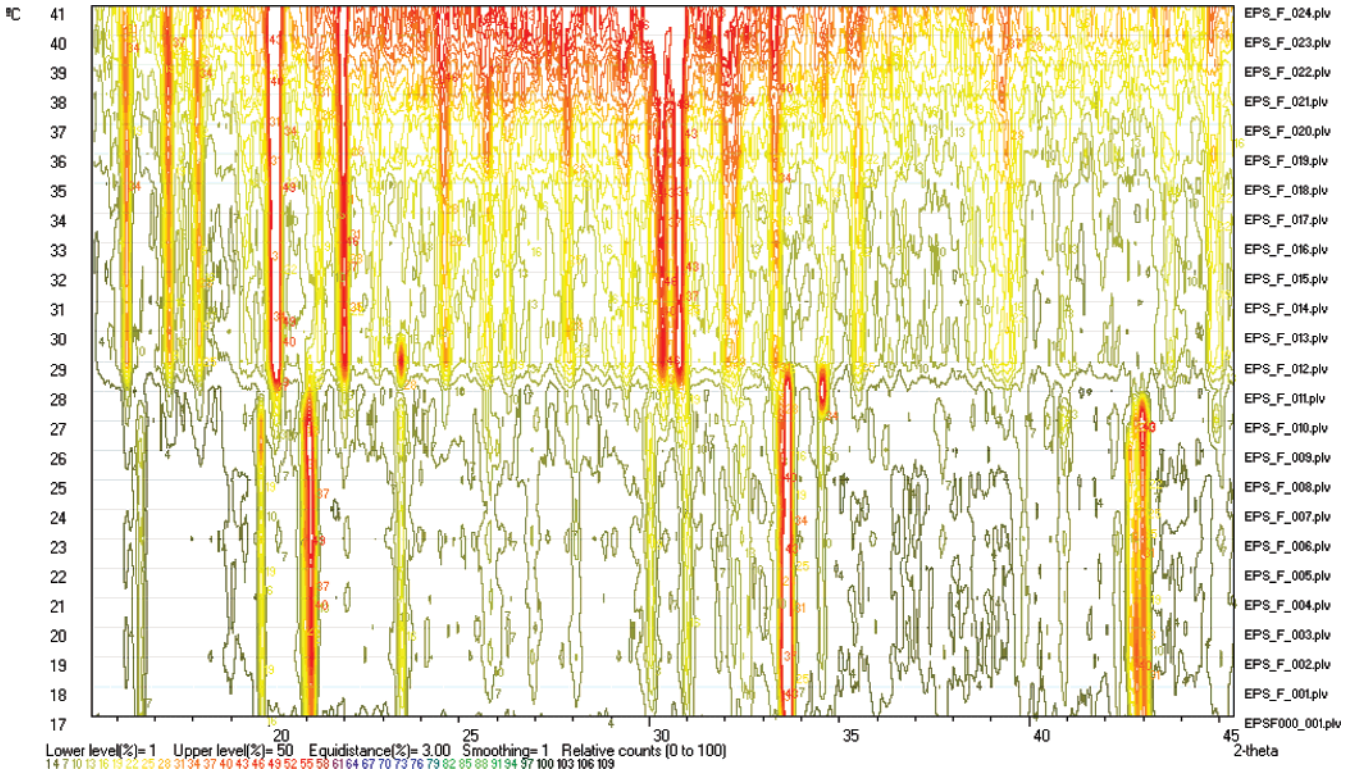

Figure 6. XRTD mapping for epsomite dehydration obtained using no filter. The strongest XRD line of epsomite appears at ~21° 2θ; the remaining strong lines above the epsomite line correspond to hexahydrite.

thenardite transition is typically reported as occurring at 32.4 °C,[24,37] and Correcher et al.[4] detected mirabilite dehydration at ~29 °C but without specifying the RH. Dehydration of sodium and also magnesium sulfates is strongly dependent on RH. Scattered data on equilibrium RH of the $Na_2SO_4 + H_2O$ system at a given T are also found in the literature. Thus, thenardite is referred to as the stable form below 80.7, 86.9, or 91.4% RH at 25 °C according to different authors.[7,25] Moreover, it is reported that when RH falls below 71% at 20 °C, mirabilite dehydrates rapidly to thenardite.[38−40]

Regarding the $MgSO_4 \cdot nH_2O$ series, the naturally occurring members are epsomite ($MgSO_4 \cdot 7H_2O$), hexahydrite ($MgSO_4 \cdot 6H_2O$), and kieserite ($MgSO_4 \cdot H_2O$).[11] Like mirabilite, epsomite dehydration is strongly dependent on RH and so the reported values of epsomite dehydration toward hexahydrite are varied given that measurements were performed under different conditions. According to García-Ginea et al.,[2] epsomite transforms (reversible reaction) to hexahydrite above 28 °C (unknown RH). Vaniman et al.[6] found that epsomite transforms readily to hexahydrite at ~25 °C at 50−55% RH and at lower T as water activity decreases. The sometimes contradictory results of the many studies of the subject confirm the rather complex behavior of these sulfate salts.

Though morphological studies of mirabilite−thenardite dehydration using ESEM are key to visualizing how the reaction proceeds,[26] investigation of the process by XRTD has proven to be a powerful analytical tool to better understand this complex process.[4,7] Our XRTD results, in the form of mappings, reveal that the use of a filter in thermodiffraction improves the quality of the new formed phase diffraction patterns; i.e., less amorphous compounds are generated. When the filter is used, phase transition is principally driven by the thermal energy from the lamp, since the precursors block direct impact of the radiation. Mirabilite and epsomite therefore mainly undergo thermodehydration. However, it cannot be ruled out that the lower RH imposed in this experiment can synergistically favor the dehydration process. Thus, dehydration of thermally stimulated mirabilite at ~27 °C agrees better with the 29 °C transition T reported by Correcher et al.[4] than the 32.4 °C equilibrium T.

On the other hand, the intense radiation emitted by the lamp without the filter impacts directly on the precursors. In the case of the mirabilite, dehydration starts immediately after initial exposure, i.e., during the first thermodiffractogram. The intense irradiation catalyzes dehydration by raising the T of the sample. That is, the absorption of radiation by the sample causes an additional thermal effect, here termed a photodehydration process. Surprisingly, our results disclosed quite different radiation behavior for epsomite, given that dehydration toward hexahydrite occurs at approximately the same T as when the filter is used, which suggests that epsomite is less susceptible to radiation damage.

Given that the halogen lamp mainly emits in the visible−infrared spectrum, we may hypothesize that dehydration of the analyzed sulfates is principally triggered by exposure to very intense irradiation (similar to flash bulbs). Although the UV emission detected was very low, we cannot discount some UV

(37) Winkler, E. M.; Singer, P. C. *Geol. Soc. Am. Bull.* **1972**, *83*, 3509−3514.
(38) Sperling, C. B.; Cooke, R. V. *Earth Surf. Processes Landforms* **1985**, *10*, 541−555.
(39) Charola, A. E.; Weber, J. In *Proceedings of the 7th International Congress on Deterioration and Conservation of Stone*; Delgado Rodríguez, J., Henriquez, F., Jeremias, J. T., Eds.; Laboratorio Nacional de Engenharia Civil: Lisbon, 1992; Vol. 2, pp 581−590.
(40) Benavente, D.; García del Cura, M. A.; García-Guinea, J.; Sánchez-Moral, S.; Ordóñez, S. *J. Cryst. Growth* **2004**, *260*, 532−544.

damage to the salts. In fact, Mars[41] already suggested that UV radiation can cause mineral dehydration. Yen et al.[42] found that UV radiation was capable of increasing the dehydration rate of goethite in high-vacuum conditions. Thermal and radiation stability of epsomite and mirabilite under Europa (Jovian moon) environmental conditions has also been studied.[30] It was found that mirabilite is less thermally stable than epsomite and that the activation energy for dehydration of mirabilite (0.45 ± 0.05 eV) is lower than for epsomite (0.90 ± 0.10 eV). Though extrapolation is not feasible since the low-T and ultra-high-vacuum conditions on Europa are quite different from those of our experiments, the results agree with our findings, in the sense that mirabilite is more sensitive than epsomite to dehydration under external stimulation.

It is remarkable that direct exposure of both mirabilite and epsomite to high-intensity radiation accelerates their dehydration kinetics. This has important implications for heritage conservation, since the faster the dynamics of mineral transformation, the worse the damage in the salt-loaded support, because of crystallization pressure on the substrate. The presence of an amorphous phase during the mirabilite−thenardite transition in both thermally and photoinduced dehydration allows us to consider that mirabilite dehydration always occurs through an amorphous-mediated, solid−solid conversion. Likewise, thenardite hydration toward mirabilite has been demonstrated by ESEM to proceed through thenardite dissolution followed by precipitation of mirabilite, instead of a direct hydration of thenardite.[43,44] Regarding epsomite dehydration toward hexahydrite, data suggest that in both XRTD procedures a solid−solid reaction occurs with no amorphous-mediated step.

Crystal Chemical Insight into Dehydration Reactions. To explain the dehydration behavior of mirabilite and epsomite from a structural and crystal chemical point of view, we have used the approach proposed by Gutmann[45] based on variations of inter- and intramolecular interactions. This approach has been successfully applied to solid-state phenomena, such as crystal growth, silicate reactivity, solid−water interfaces, bond-length variations in minerals under high pressure, epitaxy phenomena, relations between structure, reactivity, and microcrystalline size, and adsorption and surface layer phenomena in general.[46] The studied hydrated sulfates can be considered as structures consisting of SO_4 and H_2O molecular fragments, joined together by hydrogen bonds, as well as cations (Na or Mg, respectively, in mirabilite and epsomite). These cations are octahedrally coordinated by H_2O molecules with relatively weak bonds between cation and oxygen atom. The Mg−O bond is stronger than the Na−O bond, with Na−O distances between 2.39 and 2.47 Å in mirabilite[47] and Mg−O distances between 2.05 and 2.10 Å in epsomite.[48] Moreover, it is the occurrence of Mg in the structure of the hydrated sulfate, rather than the less electronegative Na cation, that makes intermolecular interactions stronger and the S−O and H−O bonds of SO_4 and H_2O molecular fragments weaker.

Table 1. Physicochemical Properties of Mirabilite and Epsomite[a]

	solubility (g/100 mL in cold water)	density (g/cm^3)	refraction index
mirabilite	11.0	1.46	1.391−1.398
epsomite	71.0	1.68	1.433−1.461

[a] Data from ref 49.

Structural and crystal chemical controls of physicochemical properties are evidenced by the clearly different densities, refraction index, and solubilities measured for these two hydrated sulfates (Table 1), in spite of their thermal behavior. The density, refraction index, and solubility of epsomite are higher than in mirabilite.[49] Strong intermolecular interactions allow higher structural packing, explaining the higher density observed in epsomite. Structural packing allows other intermolecular interactions, in addition to hydrogen bonds, such as second-nearest neighbors weak O−O orbital interactions, responsible for the observed increase in refraction index and solubility. Reduction of O−O distances and increasing electronic overlap among oxygen atoms produce a broadening of the valence band, mainly formed by contribution of oxygen atoms. This increase of the highest occupied molecular orbital (HOMO)[50] involves an increase in the softness of the oxygen ions and favors a stronger orbital interaction with low-lying acceptor hydrogen orbitals of aqueous media or lowest unoccupied molecular orbital (LUMO). We propose that the stronger "intermolecular interaction" responsible for the higher solubility of epsomite is also responsible for its higher thermal stability than mirabilite.

CONCLUSIONS

This paper demonstrates that modified OSXRD is a suitable technique to investigate thermodehydration and photodehydration of heat- and photosensitive hydrated salts like mirabilite and epsomite. In situ study with this technique, together with the new routines for 2D mapping, offers new insight to better interpret the reaction trends and kinetics of the dehydration of mirabilite and epsomite. Overall, as radiation is very effective at breaking chemical bonds, it speeds up the chemical reaction of the minerals' dehydration. For mirabilite, phase transition occurs at lower T than thermal damage, whereas this behavior is not observed for epsomite. Data confirm that mirabilite is thermally and radioactively less stable than epsomite. Thermal and photoinduced dehydration of mirabilite is a non-isothermal reaction occurring through an amorphous-mediated step. Epsomite thermodehydration is also a non-isothermal reaction, though photodehydration is an isothermal process, both reactions proceeding as true solid-state reactions.

The implications of this study for cultural heritage conservation are significant. When hydrated salts are involved in the alteration

(41) Huguenin, R.; Prim, R. G.; Maderazzo, M. *Icarus* **1977**, *32*, 270−298.
(42) Yen, A. S.; Gellert, R.; Schroeder, C.; et al. *Nature* **2005**, *436*, 49−54.
(43) Rodríguez-Navarro, C.; Doehne, E. *Earth Surf. Processes Landforms* **1999**, *24*, 191−209.
(44) Golcalves, T. D.; Rodrigues, J. D.; Abreu, N. H. *J. Cult. Heritage* **2006**, *7* (3), 193−200.
(45) Gutmann, V. *The donor-acceptor approach to molecular interactions*; Plenum Press: New York, 1978.
(46) Jensen, W. B. *The Lewis Acid-Base Concepts: An Overview*; John Wiley & Sons: New York, 1980
(47) Levy, H.; Lisensky, G. C. *Acta Crystallogr., B* **1978**, *34*, 3502−3510.
(48) Baur, W. H. *Acta Crystallogr.* **1964**, *17*, 1361−1369.
(49) *CRC Handbook of Chemistry and Physics*; CRC Press: Boca Raton, FL, 2005.
(50) Tossell, J. A.; Vaughan, D. J. *Theoretical Geochemistry: Applications of quantum Mechanics in the Earth and Mineral Sciences*; Oxford University Press: Oxford, 1992.

processes of art works, the conservation policy is to maintain constant environmental conditions, otherwise crystallization−dissolution and hydration−dehydration processes can occur leading to crystallization pressures that ultimately cause breakage of their supports. Thus, accurate knowledge of the environmental conditions at which dehydration transition occurs for each particular salt, as well as a mixture of salts, is crucial to adopt the precise strategies to prevent further deterioration. At present, art work deterioration by salt weathering is limited by setting RH and *T* values within "safe ranges" in which paintings in museums and caves, polychrome ceramics, or sculptures, etc., are exposed. The results presented here provide a better understanding of how damage caused by dehydration of sulfate salts results from direct exposure to intense radiation and not only from *T* and RH changes. This means that these salts are both heat and radiation sensitive. Given that flashbulbs produce a burst of light that contains both long- and short-wavelength radiation (UV and IR radiation) besides heat, it is proposed that flashes can favor the dehydration of determined hydrated salts. In other words, flashes would catalyze the chemical reactions that ultimately can cause artwork deterioration by salt weathering. The implications of this finding go further, since for the purposes of research and conservation of the cultural heritage art works are bombarded with visible and invisible shorter wavelength light, such as that used in infrared reflectography, etc., that have up to now been considered nondestructive analytical techniques, although recently their innocuousness has been questioned.

ACKNOWLEDGMENT

This research was financed by the Andalusian Research Group RNM-0179, the Research Project BTE 2003-07867-CO2-O1 (SEUID-MCT, Spain) and a research contract from the Junta de Andalucia awarded to C.C. We thank Angel Caballero for his technical drawing.

Received for review December 21, 2006. Accepted April 12, 2007.

AC062412H